Generating of short ultrasonic pulses using active damping

J. Rautenberg, S. Olfert, B. Henning[1]

[1]University of Paderborn, Germany, E-Mail: Henning@emt.upb.de

Abstract

In non-destructive testing (NDT) with ultrasound the emission of short pulses is essentially if the echoes of nearby obstacles should be separated from the emitted signal.

In this contribution a new approach is shown how to generate a short ultrasonic pulse using a 3−1 composite transducer. Therefore the ceramic bars, which are embedded in a polymer matrix, will be regarded as an exciter for the entire structure. After the pulse excitation the same bars can also be used for active damping to increase the bandwidth of the entire system. The Mason model serves as a basis for the description of the ultrasonic transducer and is extended to the composite structure. The excitation signal is adaptively modified by a suitable signal processing. Therefore the changes of boundary conditions, like the ambient temperature or acoustic impedance of adjacent media are considered.

Key words: Mason model, composite transducer, pulse generation

Introduction

Short ultrasound pulses are necessary in many areas of ultrasound measurement. In the non-destructive testing of materials a short pulse is needed to separate the echoes of nearby targets. For the identification of material parameters short pulses are needed to identify different paths of wave propagation [1].

There are well known techniques like mechanical damping, series- and parallel-tuning or the acoustic impedance match of the transducers backing to achieve short ultrasonic pulses [2]. In general these approaches decrease the amplitude of the transmitted pulse and they are not suited for the composite material as its acoustic impedance dramatically changes with frequency. In this contribution a 3−1 composite transducer is used to generate an ultrasonic pulse that is as short as possible even if the acoustic impedance of the target medium changes. Therefore, it is excited with an adapted signal taking into account the adjacent media properties and multiple reflections as well as the interconnection between the composite materials.

A modified Mason model will be introduced which enables the signal processing for short pulse excitation. Some examples will demonstrate the use for high and low impedance specimens without changing the matching layer of the transducer.

Theory

The aim is to realize signals which are as similar as possible to the one- or two-sided ideally matched transducer. The pulse responses of such transducers consist of 3 or 2 single pulses (figure 1) [2], [3]. At bandwidth limited excitation with the centre frequency $f_0=1/T$ odd or even signals arise (figure 2).

If there is an acoustic mismatch a feedback of adjacent media interferes with the pulse responses of figure 1, but it appears always after the first two pulses. The interference does not affect the first part of the envelopes in figure 2. The modelling of an ideal envelope gets possible. It is the

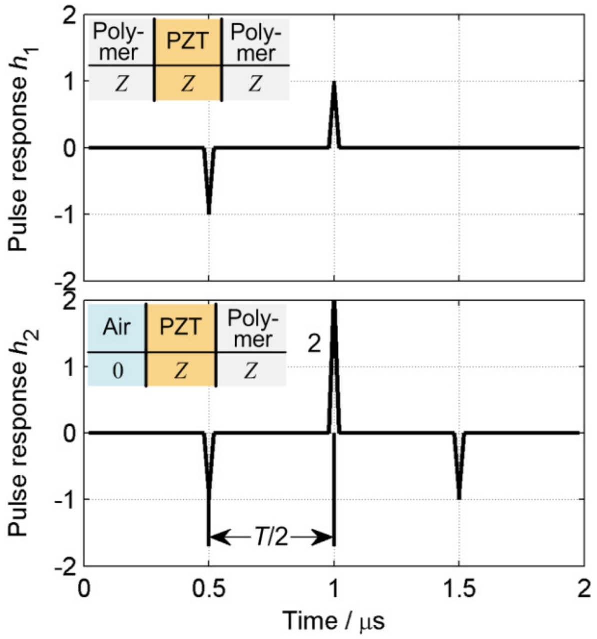

Figure 1: Ideal pulse response of a two-sided ideally matched transducer (top) and of an one-sided ideally matched transducer (bottom).

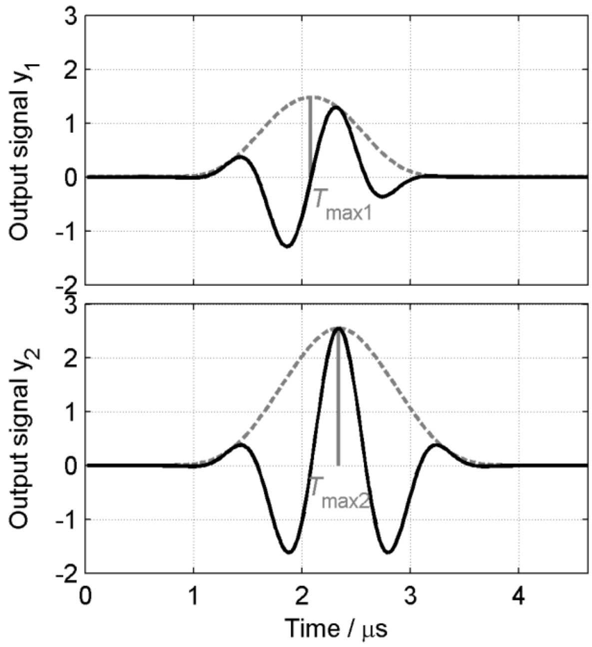

Figure 2: Bandwidth limited pulse response of a two-sided ideally matched transducer (top) and of an one-sided ideally matched transducer (bottom).

mirrored first half of a measured signal's envelope:

$$y_{h,ideal}(t)=\begin{cases}\mathrm{env}\{y(t)\} & 0<t<T_{\max}\\ \mathrm{env}\{y(T_{\max}-t)\} & T_{\max}\le t\end{cases} \qquad (1)$$

By suitable modelling and signal processing the measured signal's envelope shall be fit to this ideal envelope.

Modelling

As a basis for the modelling the Mason model is used [4]: An electrical excitation is transformed into two waves v_0 and $-v_0$ at each boundary $x=\pm d/2$ of a piezoelectric material, propagating in opposite directions. At every boundary layer b/a or b/c these waves are reflected in the source medium b and transmitted in the adjacent media. The initial amplitude ratios (not the signs) of the four waves can be described by the transmission coefficient D:

$$\left.\begin{array}{ll}\text{Wave in medium a:} & D_{\mathrm{ba}}=\dfrac{2Z_{\mathrm{a}}}{Z_{\mathrm{a}}+Z_{\mathrm{b}}}\\ \text{Wave 1 in medium b:} & D_{\mathrm{ab}}=\dfrac{2Z_{\mathrm{b}}}{Z_{\mathrm{a}}+Z_{\mathrm{b}}}\end{array}\right\}\text{on the pos. } x=-\frac{d}{2}$$

$$\left.\begin{array}{ll}\text{Wave 2 in medium b:} & D_{\mathrm{cb}}=\dfrac{2Z_{\mathrm{b}}}{Z_{\mathrm{b}}+Z_{\mathrm{c}}}\\ \text{Wave in medium c:} & D_{\mathrm{bc}}=\dfrac{2Z_{\mathrm{c}}}{Z_{\mathrm{b}}+Z_{\mathrm{c}}}\end{array}\right\}\text{on the pos. } x=\frac{d}{2}$$

At the top of figure 3 the behaviour at a boundary layer between a passive material a und the active material b is illustrated. Beneath, the same is shown for the transmission from the active layer b to the passive layer c.

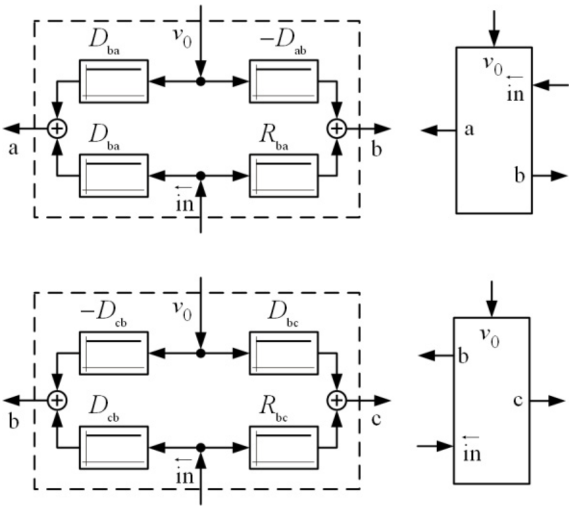

Figure 3: Transmission and reflection at the a/b-boundary (top) and the b/c-boundary of the composite layer (bottom).

Apart from v_0 there is an additional port $\overleftarrow{\mathrm{in}}$ representing the treatment of multiple reflections in the active material. R_{ba} and R_{cb} are the amplitude reflection coefficients:

$$\left.\begin{array}{ll}\text{Wave 1 in medium b:} & R_{\mathrm{ba}}=\dfrac{Z_{\mathrm{a}}-Z_{\mathrm{b}}}{Z_{\mathrm{a}}+Z_{\mathrm{b}}}\\ \text{Wave 2 in medium b:} & R_{\mathrm{bc}}=\dfrac{Z_{\mathrm{c}}-Z_{\mathrm{b}}}{Z_{\mathrm{a}}+Z_{\mathrm{b}}}\end{array}\right\}\text{on the pos. } x=\pm\frac{d}{2}$$

If the Mason model should be applied to a 3−1 composite transducer it is necessary to consider the different media of the composite one by one, their interaction and the effective material as well. Figure 4 shows the interaction of the different parts of composite material.

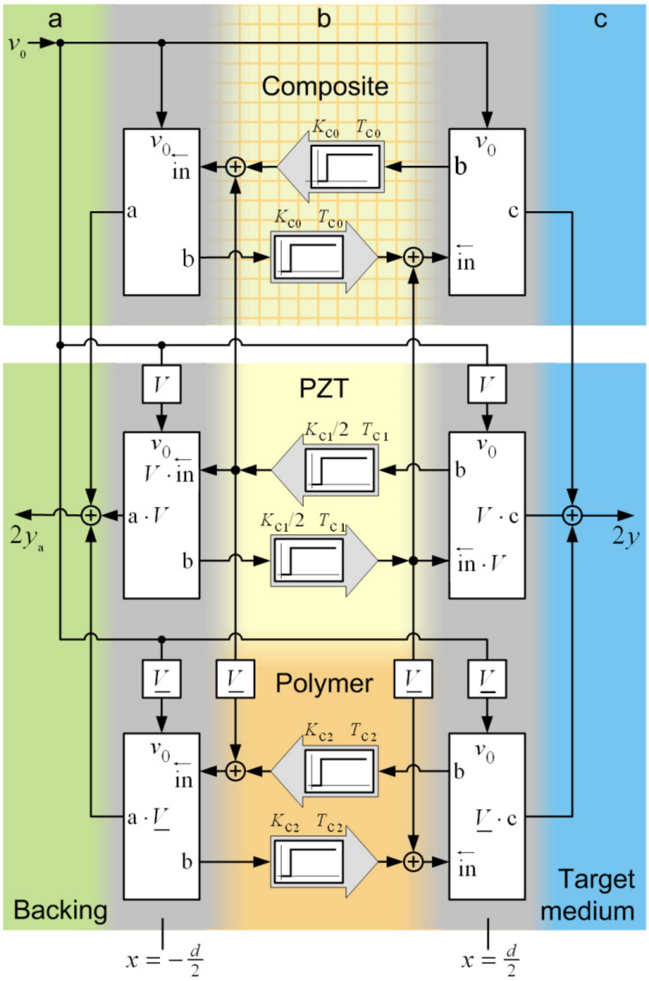

Figure 4: Model of a composite transducer.

If the bars of the piezoceramic (PZT) extend, they take along the polymer, they are embedded in whereas a coupling from the polymer to the PZT bars can be neglected. It depends on the volume fraction V of the PZT bars $(\underline{V}=(1-V))$, the size of an elementary structure in comparison to the wavelength and the material properties like density and sound velocities how the effective composite material vibrates. For the presented model the size of the structure is neglected because the composite material is well-designed by the Fraunhofer IBMT [6].

It has turned out that the described coupling at the examined composite is equal to the abovementioned volume fraction of PZT V and that the effective sound velocity can be expressed by the Hill approach, a combination of Reuss's and Voigt's theories. Therewith it is possible to determine the times $T_{c,i}$, $i = 0..2$, which the waves need to pass the composite disc. Apart from that an attenuation of the amplitude K_c was introduced to take the different energy dissipation of the materials into account.

Signal processing

The output signal in form of an average unidirectional surface velocity y can be expressed by convolution of the excitation v_0 with the pulse response h:

$$y(t) = v_0(t) * h(t) \tag{2}$$

By a specific calculation of v_0 any arbitrary waveform y can be generated if h is known. To find v_0, equation 2 is solved to v_0.

$$\begin{aligned} & y(t) = v_0(t) * h(t) = \mathbf{H} \cdot v_0(t) \\ & \Rightarrow v_0(t) = \mathbf{H}^{-1} \cdot y(t) \end{aligned} \tag{3}$$

H is the Hankelmatrix. The inverse of this non quadratic matrix does not exist so that it is merely a best square problem. With this, v_0 is the best but not the ideal solution, however.

In the practice it has turned out that with the assumption $y(t) = \delta(t)$ the result $\tilde{y}(t) = v_0(t) * h(t)$ shows good correlation: $\phi_{\tilde{y}\tilde{y}}(t) = E\{\tilde{y}(\tau - t) \cdot \tilde{y}(\tau)\} = \tilde{y}(t) * \tilde{y}(-t)$ has a maximum for a time delay $t = 0$ and is near zero else wise. Therewith it is possible to determine a kind of time-reversed pulse response $\tilde{h}(t)$ in such a way that the average surface velocity $\tilde{\tilde{y}}(t) = y(t) * \tilde{h}(t) * h(t)$ is nearly the same as the desired $y(t)$. This step is well known from the matched filter design in communication technology:

$$\begin{aligned} \tilde{\tilde{y}}(t) &= y(t) * \tilde{y}(t) * \tilde{y}(-t) \\ &= y(t) * (v_0(t) * h(t)) * (v_0(-t) * h(-t)) \\ &= y(t) * \underbrace{v_0(t) * v_0(-t) * h(-t)}_{\tilde{h}(t)} * h(t) \end{aligned} \tag{4}$$

Parameter identification

To evaluate the quality of a signal, two criteria are defined. The first criterion assesses the duration of the pulse. The area beneath the normalised envelope of the signal shall be minimal. The second criterion characterises the quality of the pulse, i.e. the deviation of the measured signal's envelope from the ideal one.

According to these criteria the transmitted signal is optimised via a genetic algorithm. For this purpose the NSGA-II algorithm [5] was adapted to the present problem. First, the mutation probability is decreased with every new generation. This procedure is well-known from the simulated annealing algorithm. Apart from that normal distributions instead of equal distributions were used for mutations as well as the generation of children. Therewith a faster convergence was obtained.

This multi-objective optimisation yields to a Pareto-frontier with respect to the abovementioned optimisation objectives (figure 5). The optimisation was repeated at different environment temperatures to analyse the temperature influence on the model parameters. Therefore, the last generation of a low temperature optimisation was migrated to a decimated initial generation for the higher temperature.

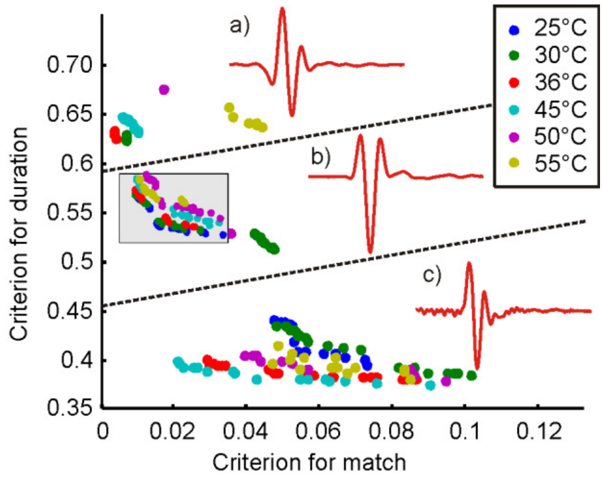

Figure 5: Optimisation results for different temperatures.

It becomes obvious that the Pareto-frontiers can be divided into three groups. In figure 5 these are separated from each other by dotted lines. Although the envelope of signal a) shows the best similarity to the ideal envelope, it is the signal of the greatest duration. Taking the receiver into account it can be shown that this is the signal y_2 of figure 2. The second group with signal b) coincides with signal y_1 of figure 2, whereas signal c) is even shorter than any signal in a conventionally damped transducer. Unfortunately this signal strongly varies with temperature. This is why signal b) was chosen. The parameter identification was repeated with a smaller domain of definition for this group (gray box in figure 5).

Results and discussion

The results are represented and discussed for two materials with acoustic impedances of 1.5 MRayl and 36.3 MRayl respectively.

The first investigated test specimen is a polymer rod with low acoustic impedance. For the excitation with a defined bandwidth a Gaussian pulse was used which is represented at the top of figure 6 in gray. For comparison the electrical excitation signal which was determined with the presented new method and which generates the shorter mechanical pulse is shown beneath. In both cases the received signals of the emitted sound waves are shown in black. It is readily identifiable that the duration of the received signal with Gaussian excitation is considerably longer.

At the circular test specimen additional waves arise from the edges of the rod which appear the more strongly the higher the mismatch of the acoustic impedances between transducer and test specimen is (cf. figure 8, high impedance material).

In bounded solids there are further waves arising due to multiple mode conversions between longitudinal and transversal waves at the boundaries. The delay time Δt between the first echo of the longitudinal wave and the transversal

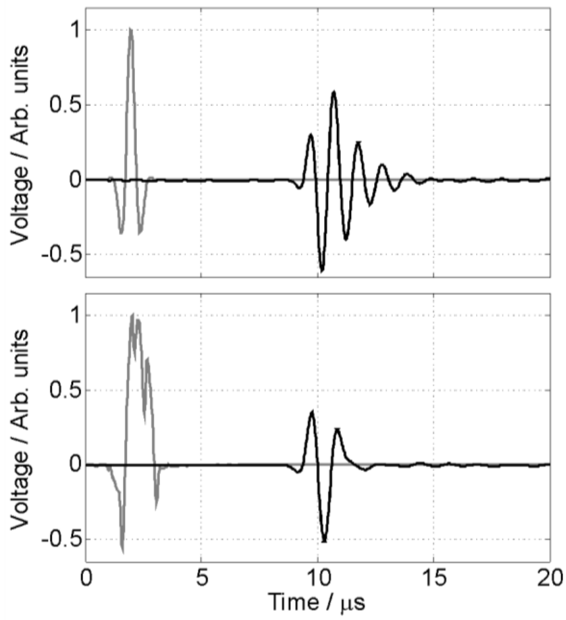

Figure 6: Transmission bulk wave measurement in a polymer rod with low impedance Z_1 without (top) and with active damping (bottom): Exciting signals (gray) and transmitted signals (black).

subsequent echo can be determined according to equation 5 if the diameter D of the test specimen and the sound velocities c_L and c_T are known:

$$\Delta t^2 = D^2 \cdot \left(\frac{1}{c_T^2} - \frac{1}{c_L^2} \right) \tag{5}$$

Figure 7 illustrates the appearance of the different described additional waves. The rays point into the direction of plane waves in the circular test specimen. These waves interfere at the receiver in a constructive way and therewith constitute the multiple echoes in a received signal.

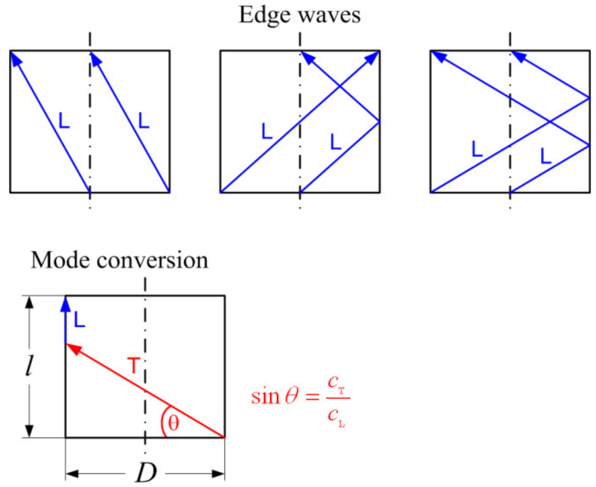

Figure 7: Ray model for the determination of different echoes at through transmission measurements in rods.

Considering the rays in the test specimen it is possible to determine the time of flight of different waves. These are shown at the top of figure 8. With this it is possible to identify the echoes in the received signal if a single echo is short enough. At the diagram of figure 8 the received signals

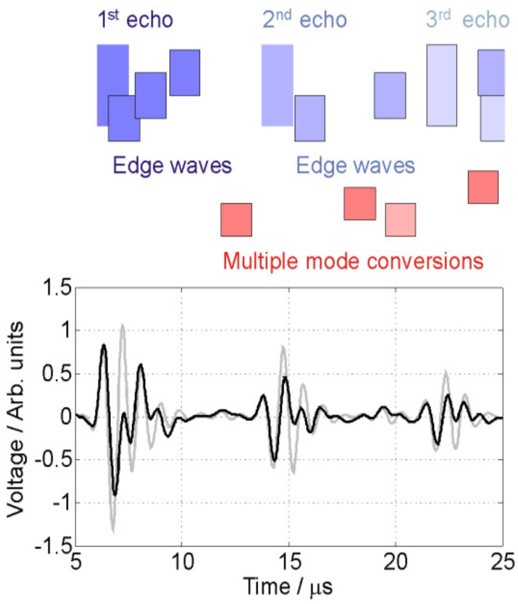

Figure 8: Transmission bulk wave measurement in a rod with high impedance Z_2 and without active damping (black/gray). Edge waves (blue) and multiple mode conversions (red) get observable.

for the high impedance specimen are shown (black: with active damping, gray: without active damping). There is a good agreement between the determined times of flight and the observed arrivals in the received signal if the new active damping is used. With Gaussian excitation the described signal parts cannot be separated simply.

Conclusion

With the presented modelling and signal processing an excitation signal can be found, wherewith the duration of a transmitted mechanical signal can be significantly reduced. So it is possible to identify single waves' echoes in transmitted signals better than with Gaussian excitation.

References

[1] J. Rautenberg, B. Henning: Simultaneous direct and indirect measurement of sound velocities, Eurosensors XXII, Dresden, 07.-10.09.2008, Proceedings

[2] Asher, R.C.: Ultrasonic Sensors. Institute of Physics Publishing, Bristol Philadelphia, 1997

[3] J. Krautkrämer, H. Krautkrämer: Werkstoffprüfung mit Ultraschall (5th ed.). Springer Verlag, Berlin Heidelberg New York, 1986

[4] Kino, Gordon S.: Acoustic waves, Prentice-Hall, Englewood Cliffs, 1987

[5] K. Deb, A. Pratap, S. Agarwal: A fast and elitist multiobjective genetic algorithm: NSGA-II. IEEE Trans. Evol. Comput. (2002), 182-197

[6] Datasheet, Piezoelektrische Composites, http://www.ibmt.fraunhofer.de/fhg/Images/sensorfertigung_piezoelektrische_13composites_tcm266-68003.pdf